

November 2009 tropical cyclone *Phyan* in the eastern Arabian Sea: Oceanic response along west India coast and Kavaratti lagoon

Antony Joseph, R.G. Prabhudesai, Prakash Mehra, Vijay Kumar, Yogesh Agarwadekar, Luis Ryan, Pradhan Rivankar, Blossom Viegas

National Institute of Oceanography, Council of Scientific and Industrial Research,
Dona Paula, Goa - 403 004, INDIA

Abstract- Spatial and temporal response of the coastal waters of eastern Arabian Sea (AS) and Kavaratti lagoon to the tropical cyclonic storm 'Phyan', which developed in the southeastern AS and swept northward along the eastern AS during 9-12 November 2009 and finally made landfall at the northwest coast of India, is examined based on time-series measurements of sea-surface wind (U_{10}), gust, gust factor, barometric pressure, precipitation, atmospheric temperature, SST, and significant wave height from satellite-derived and in-situ measurements. The maximum wind-speed (U_{10}) of ~16 m/s occurred at Kavaratti Island region followed by ~8 m/s at Dwarka in Gujarat, where the cyclone landfall occurred, and ~7 m/s at Diu located just south of Dwarka as well as two southwest Indian coastal locations at Mangalore and Malpe. All other west India coastal locations recorded maximum wind speed of ~5-6 m/s. Gust factor during peak storm event was highly variable with respect to topography, with steep hilly stations and proximate thick and tall vegetation exhibiting the largest value whereas coastal planes and Island stations exhibiting the least. Rainfall in association with Phyan was temporally scattered, with the highest 24-h accumulated precipitation (~60 mm) at Karwar and ~45 mm at several other locations. Impact of Phyan on the west India coastal waters was manifested in terms of intensified significant wave height (~3 m at Karwar, Panaji, and Ratnagiri), sea surface cooling (~5°C at Calicut), and surge flooding (~80 cm at Verem). Several factors such as (i) water piling up at the coast supported by seaward flow of the excess water in the rivers due to heavy rains and westerly cross-shore wind, (ii) water piling down at the coast supported by the northerly alongshore wind (by virtue of Coriolis effect) and upstream penetration of seawater into the rivers, and (iii) possible interaction of upstream flow with river runoff, together resulted in the observed surge flooding at the west India coast. Despite the intense wind forcing, Kavaratti Island lagoon experienced insignificantly weak surge (~7 cm) because of lack of river influx and absence of a sufficiently large land boundary required for the sustenance of wave/wind-driven water mass which tends to pile up at the land-sea interface.

I. INTRODUCTION

In the Indian Ocean rim countries, tropical cyclones rank as the highest cause of loss of lives and property damage related to natural disasters although these regions have been affected several times in the past by earthquakes and recently even tsunamis. Tropical cyclones generate quite strong wind fields and rainfall. Passage of tropical cyclones over a large surface of water (such as sea) gives rise to unusually large waves. The cyclone-generated winds cause seawater to pile up on the coast and lead to storm-surge (i.e., inundation and flooding of

low-lying coastal regions). Most of the countries located along the periphery of the North Indian Ocean are threatened by storm surges associated with severe tropical cyclones. The destruction due to the storm surge flooding is a serious concern along the coastal regions of India, Bangladesh, Myanmar, Pakistan, Sri Lanka, and Oman. Although the frequency of storm surges is less in the Arabian Sea (AS) than in the Bay of Bengal (BoB), major destructive surges have occurred along the eastern coast of the Arabian Sea as well, particularly the coast of Pakistan and that of Gujarat (India). In this study, we use remotely sensed atmospheric, sea-state, and sea surface temperature data as well as in-situ based real/near-real time reporting surface meteorological, sea-level, and sea-state data to examine the effects of the tropical cyclone Phyan on the west coast of India and Kavaratti Island in the eastern AS.

II. DATA COLLECTION SCHEMES

A. Satellite-derived Measurements

Because of limited in-situ measurement locations, sea-surface wind (U_{10}), sea-surface waves (significant wave height), and sea surface temperature (SST) were extracted from remotely sensed satellite-derived measurements from a chain of selected locations (Fig. 1). Time-series satellite-derived wind speed measurements from twelve west India coastal water locations during the passage of the cyclonic storm indicate that the maximum wind-speed (U_{10}) of 8 m/s occurred at Dwarka in Gujarat, where the cyclone landfall occurred, followed by ~7 m/s at Diu located just south of Dwarka as well as two southwest Indian coastal locations Mangalore and Malpe. All other western coastal Indian locations recorded the maximum wind speed of ~5-6 m/s. The wind was primarily northwesterly. Spatial distribution of the wind speed maxima along twelve west India coastal waters during the passage of *Phyan* (Fig. 2) provides an indication of the gradual intensification of wind speed maxima from the southwestern region of India until Mangalore region followed by its gradual weakening from Mangalore region to Ratnagiri region, and its subsequent renewed intensification from Ratnagiri region until its landfall location on the Gujarat coast of the northeastern AS. Time-series satellite-derived wave

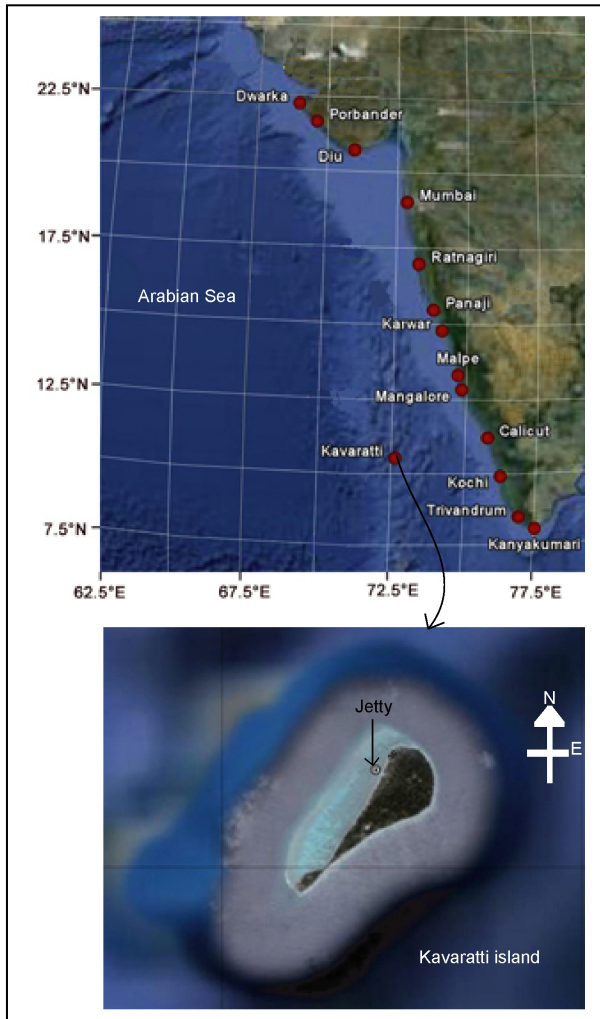


Fig. 1 Location map of surface-wind, waves, and SST measurements along the west coast of India and from Kavaratti Island region during the passage of tropical cyclone 'Phyan'.

height measurements from twelve west India coastal water locations during the passage of the cyclone indicate that the maximum significant wave height of ~3 m occurred at Karwar (Karnataka State), Panaji (Goa State), and Ratnagiri

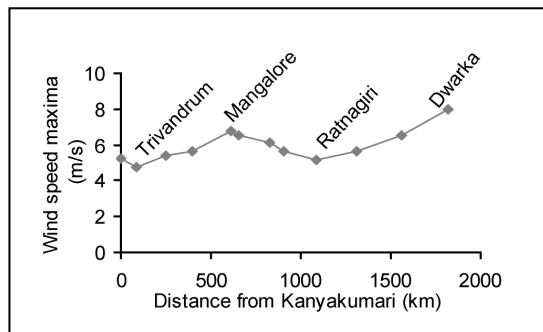


Fig. 2 Spatial distribution of the wind speed maxima along twelve west India coastal water locations during the passage of Phyan.

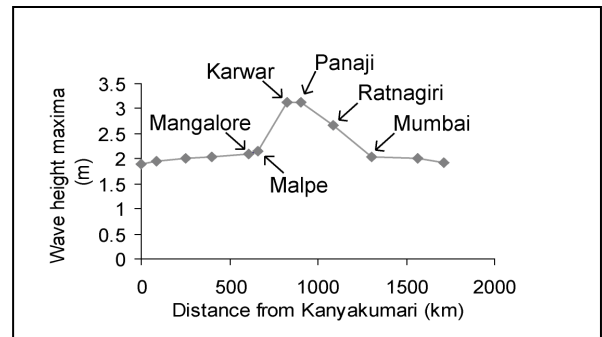


Fig. 3 Spatial distribution of the significant wave height maxima along twelve west India coastal water locations during the passage of Phyan.

(Maharashtra State) and 2 m at all other west India coastal regions. Spatial distribution of the significant wave height maxima along twelve west-India coastal water locations during the passage of Phyan (Fig. 3) depicts the distinctly large sensitivity/tendency of Karwar (Karnataka) and Panaji (Goa) regions to sea surface wave intensification, followed by Ratnagiri in Maharashtra. Phyan caused drop in SST in several regions. However, SST at Kanyakumari region, where a low pressure area formed on 7th November 2009 in association with the cyclone genesis, did not reveal a noticeable drop in SST. As evidenced from the spatial distribution of SST drop along the west India coastal waters during the passage of the cyclone (Fig. 4), the largest drop occurred at Calicut and the smallest at Kanyakumari and Porbander.

III. IN-SITU MEASUREMENTS

A. West India Coastal Locations

In-situ measurements from the west India coastal stations of Kochi, Malpe, Karwar, Goa, and Ratnagiri as well as Kavaratti Island in the Lakshadweep Archipelago in the southeastern Arabian Sea were made with the use of an Internet-accessible real/near-real time reporting Integrated Coastal Observation Network (ICON) designed, developed and established by the National Institute of Oceanography (NIO) of India, whose output can be viewed at <http://inet.nio.org>. Subsurface pressure sensors and downward-looking microwave radars are incorporated in the

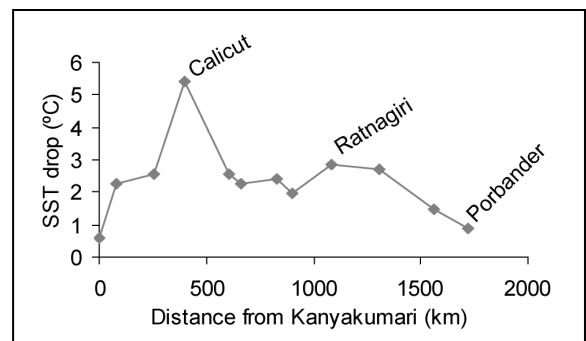


Fig. 4 Spatial distribution of SST drop along twelve west India coastal waters during the passage of Phyan

sea-level station network. The latter is a relatively new sensor, which is insensitive to variations in installation site conditions such as air temperature, humidity, and rainfall. All the devices used in the network have linear response over the full range of interest, which is a requirement most needed to avoid under-estimation of relatively large signals that occur during considerably disturbed meteorological and oceanogenic events such as storms, storm-surges, and tsunamis. Both sea-level and surface meteorological (Met) stations are powered from 12-volts batteries, which are charged through solar panels. Sea-level, Met, and surface wave parameters are acquired using dedicated Linux based data loggers and uploaded to an Internet server at 5-, 10- and 30-min intervals, respectively with the use of GPRS cellular modems. The ICON provides graphical presentation of sea-level information (observed sea-level, predicted tide, residual sea-level); significant wave height and wave direction; and Met information (vector-averaged wind speed & direction, gust (i.e., the largest wind speed amongst an ensemble of 60 samples that are measured during the 10-minute sampling span), barometric pressure, atmospheric temperature, solar radiation, relative humidity, and rainfall). Installation of sea-level sensors free from the influence of stilling-wells and long narrow tubes renders the measurements ideal for storm-surge studies by preventing waveform distortion and non-linearity of large-amplitude short-period signals.

All the five coastal locations from which in-situ measurements are available exhibited barometric pressure drop during the passage of the cyclone. Spatial distribution of the pressure drop along these five locations during the passage of the cyclone (Fig. 5) clearly indicates the trend of the pressure drop increasing in the northward direction along the coast. The 10-min vector-averaged wind speed and gust values acquired at 10-min sampling interval together with the gust factor shows the gusty nature of the wind regime during the cyclone. Spatial distribution of gust maxima (Fig. 6a) indicates the distinctively large gusty nature of wind at Ratnagiri (~30 m/s) during the currency of Phyan in contrast to the considerably smaller gust (10-14 m/s) observed at all the other stations considered in the present study. Interestingly, the gust factor maxima (Fig. 6b) indicates a different trend in which while

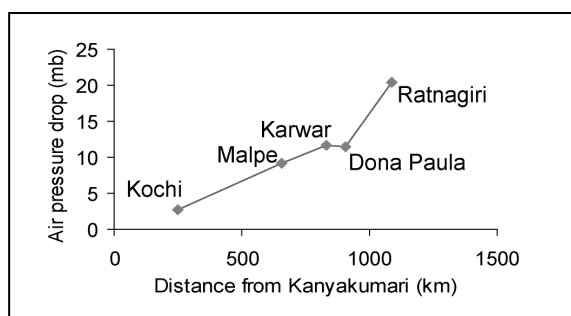


Fig. 5 Spatial distribution of the barometric pressure drop along five west India coastal waters during the passage of Phyan

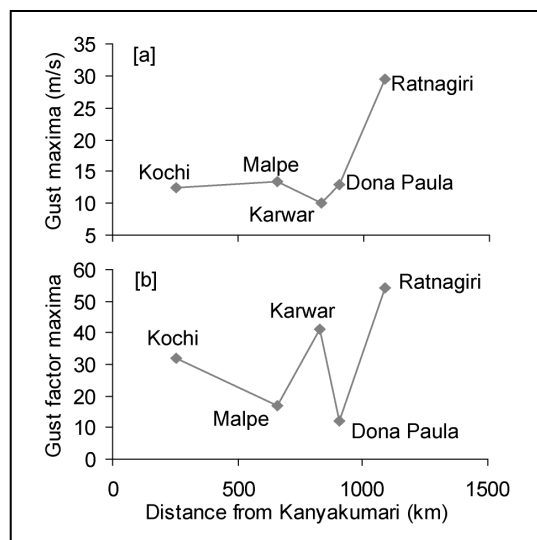


Fig. 6 Spatial distribution of [a] gust maxima and [b] gust factor maxima along five west India coastal waters during the passage of Phyan

Ratnagiri topped the gust factor maxima (~55) followed by Karwar (~40) and Kochi (~32), Malpe and Dona Paula (Goa) exhibited the least gust factor (~15). Stick-plots of the wind velocities at these coastal regions indicate the predominantly northwesterly wind field during Phyan. Rainfall data available from Kochi (in the south) and the Konkan regions covering Malpe, Karwar, Goa, and Ratnagiri during November provide an indication of the temporal distribution of the unusually large precipitation level (i.e., 24-h cumulative rainfall) at these stations in association with the Phyan. The corresponding spatial distribution (Fig. 7) illustrates that Karwar stands out distinctively as a region which experienced the largest rainfall in contrast to its neighboring coastal regions during Phyan. Kochi region experienced the least amount of rainfall during the cyclonic storm. Atmospheric cooling and spatial distribution of air temperature drop (Fig. 8) along five west India coastal regions in association with the tropical cyclonic storm indicates that Karwar and its proximate regions of Malpe and Dona Paula (Goa) experienced the maximal cooling. Surface meteorological forcing such as barometric pressure gradient, wind stress and gust; oceanographic effects such as waves, currents, and tides; and topographic effects such as bathymetry, coastal features etc. together with possible nonlinear interaction among various parameters resulted in an enhanced sea level elevation (i.e., positive surges) at the west India coastal locations (Fig. 9).

B. Kavaratti Island Region

Installation of a new surface meteorological station (NIO-AWS) at Katchery jetty in the Kavaratti lagoon immediately prior to the occurrence of Phyan provided a fortuitous opportunity to examine the surface meteorological features at this region in association with the cyclonic storm. In-situ measurements at this lagoon (Fig. 10) indicate the intensified winds (Fig. 10a, d) and barometric pressure drop (Fig. 10g)

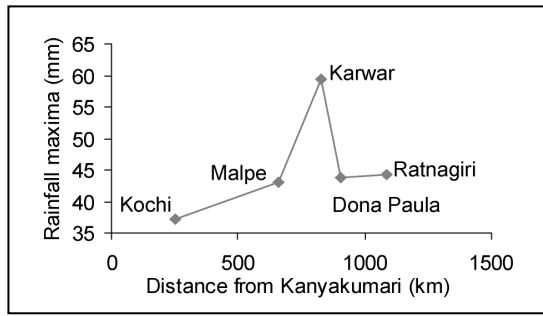


Fig. 7 Spatial distribution of 24-hr cumulative rainfall maxima along five west India coastal waters during the passage of *Phyan*

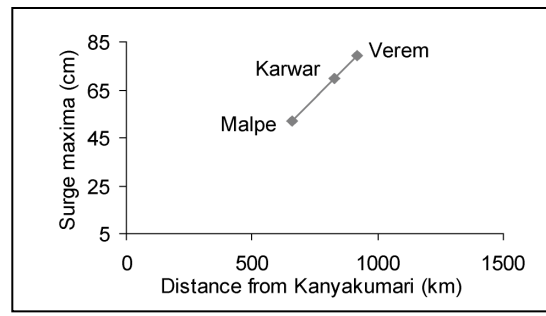


Fig. 9 Spatial distribution of surge maxima along three west India coastal locations during the passage of *Phyan*

that developed over this island in the Lakshadweep Archipelago and its proximate regions in the eastern Arabian Sea. However, no discernible atmospheric temperature drop was indicated (Fig. 10f). The wind field at Kavaratti region in association with *Phyan* was southwesterly, which is at variance with the predominantly northwesterly wind experienced at all the west India coastal locations. An interesting observation is the negligible gust factor (Fig. 10b) during the passage of *Phyan*, which is distinctly at variance with the usually large gust factor at this location. A downward-looking microwave radar gauge installed by NIO at Katchery jetty provided sea level measurements at 5-minutes interval. The observed surge maximum was ~10 cm (Fig. 10h).

IV. DISCUSSION OF RESULTS

To a first order approximation, the spatial pressure gradient associated with a cyclone primarily determines the storm-related wind field. According to the existing notion, the largest wind speeds occur in the areas where the passing cyclone further tightens the ambient pressure gradients. Such forcing across the sea water regions generates intensified sea surface waves, water currents, storm surges and associated low-land inundation, and under supportive circumstances gives rise to upwelling in the sea which results in enhanced sea surface cooling. As in [1], forcing factors of cyclogenesis interact nonlinearly, over small areas, or over a limited period during the storm development.

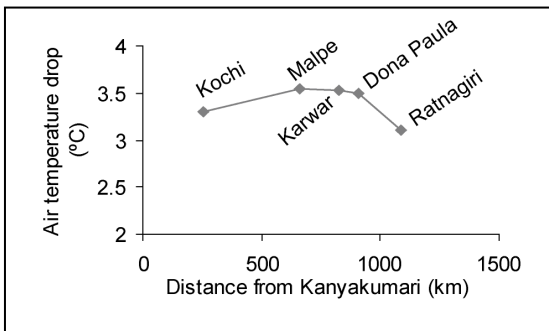


Fig. 8 Spatial distribution of air temperature drop along five west India coastal locations during the passage of *Phyan*

A. Atmospheric Pressure Gradient and Winds

The passage of *Phyan* was associated with a well-marked barometric pressure drop, whose spatial distribution (Fig. 5) clearly indicates its intensification in the northward direction along the coast. The cyclonic storm, which could have primarily been the result of the strengthened synoptic scale pressure gradient, was found to be associated with unusually large surface winds and gusts (Fig. 6). The observed strong variability of wind gusts could be associated with a downward mixing of upper-level higher wind speeds to the surface and/or the lateral spreading of convective downdrafts caused by evaporating rain in the convective storms. These observations imply that the maximum gust could be a result of a destabilization of the lower troposphere during the passage of *Phyan*. Unfortunately, no upper-air soundings during the passage of the cyclone are available to corroborate this inference. A closer examination of Fig. 6 reveals a strong station-to-station variability with respect to the maximum observed winds and gusts during the passage of the cyclone. The wind gust factor (*i.e.*, gust-to-speed ratio) provides a quantitative measure of the gustiness of the wind field (*i.e.*, wind occurring in pulses rather than in a steady fashion). It is found that during *Phyan* the gust factor registered a peaking trend at some locations and a reverse trend at some other locations. For example, whereas the gust factor increased considerably at Kochi, Karwar, and Ratnagiri during the passage of *Phyan*, it decreased considerably at Malpe and Goa. Among those stations from which in-situ time-series wind data are available, the maximum gust factor of ~60 was noticed at Ratnagiri, followed by ~40 at Karwar, and ~30 at Kochi during peak cyclone winds. Surprisingly, gust factor at Malpe (Karnataka) and Dona Paula (Goa) during peak winds are ~15. Gust factor at Kavaratti Island during peak winds is <2 (See Fig. 10). Both Ratnagiri and Karwar, which witnessed the largest gust factor, are stations located on steep hills. However, Malpe and Kochi are coastal plane areas and Kavaratti is a small island in the open sea. Dona Paula is neither plane nor a steep hilly location. From the above description it is found that the gust factor during peak storm event is highly variable with respect to topography, with steep hill stations exhibiting the largest gust factor whereas coastal planes and Island station exhibiting the least. However, Kochi station, which is located

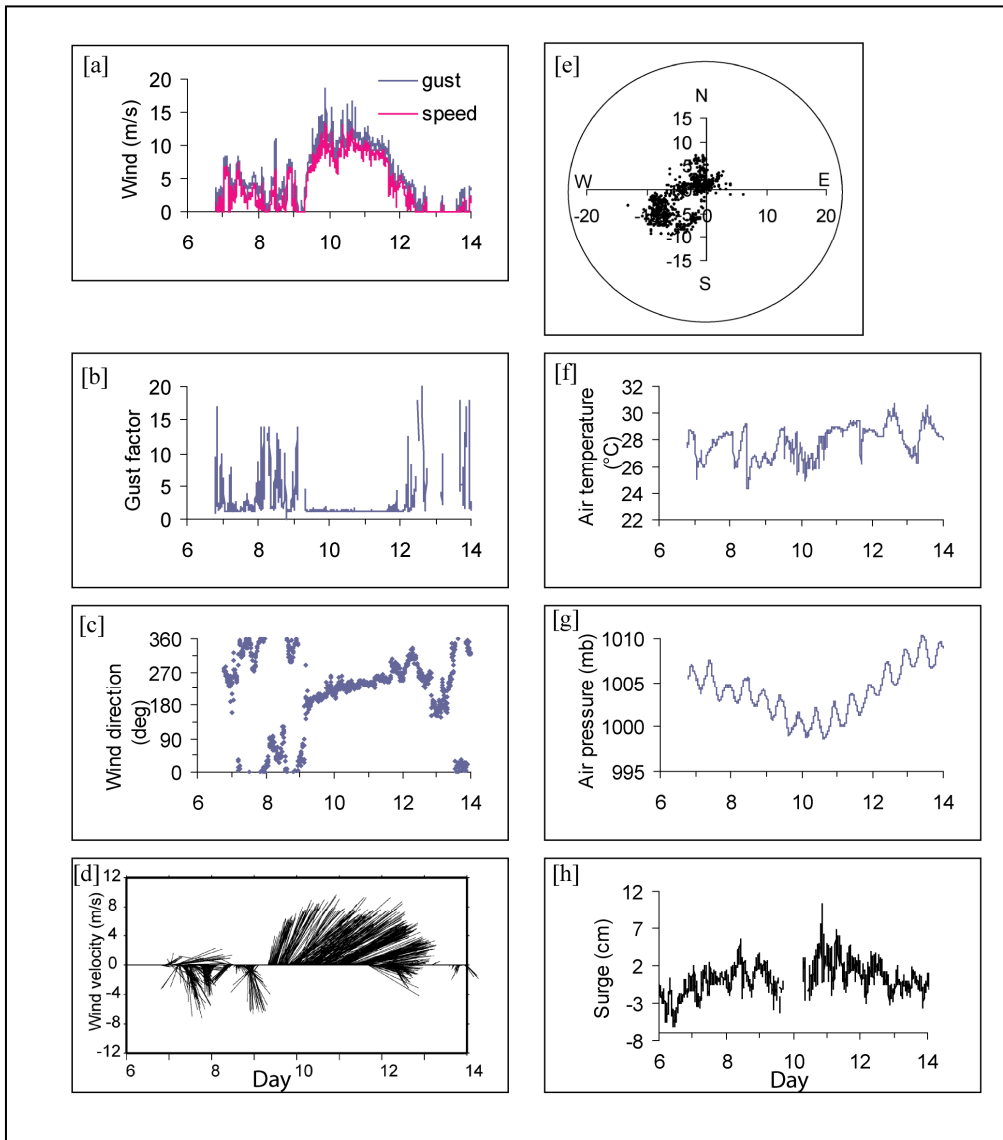


Fig. 10 In-situ measurements of the surface meteorological and storm surge features at the Kavaratti Island lagoon during the passage of Phyan.

right on the beach, exhibiting a fairly large gust factor (~ 30) during peak cyclone winds is a contradiction. Perhaps, the presence of coconut palms in the vicinity of the anemometer must have contributed in some way to the observed fairly large gust factor. As noted in [2], these results could be indicative of the considerable influence of macro-meteorological (*i.e.*, orography) or micro-meteorological (*i.e.*, trees, buildings, etc.) environmental conditions of the stations on the gust factor, a peculiarity observed only during storm conditions.

B. Precipitation and Atmospheric Cooling

Fast sampled (10-min sampling interval) in-situ measured rainfall data were available from a few locations, which

allowed examination of the spatial characteristics of the cyclone-induced rainfall distribution. The rainfall associated with Phyan was temporally scattered, with the highest value of 24-h accumulated precipitation observed at Karwar (60 mm); followed by Ratnagiri, Dona Paula and Malpe (~ 45 mm); and the least at Kochi (~ 37 mm). However, torrential rain was absent at all the locations. As the cyclone storm moved forward approximately in the northward direction and inclined towards the west India coast, arrival of the cyclone-associated rainfall also followed this pattern, occurring first at the southern region and subsequently at the next northerly locations in a step-by-step fashion. Although November falls under the Indian winter monsoon period, rainfall was totally absent at these stations during the few days preceding the cyclone. The temporal and spatial distribution of the 24-h accumulated cyclone-associated rainfall, with the hill-

dominated stations receiving substantially more rainfall, provides an indication that the amount and distribution of rainfall depends not only on the distribution of convection within the cyclone but also on orographic lifting effects. Distribution of convection and rainfall in a tropical cyclone has certain characteristic patterns both when it is over open ocean [3] and when making landfall [4]. Abundant moisture supply, resulting from the proximity of these stations to the cyclone track could be another reason for the substantially enhanced rainfall at these stations. Similar inferences have been drawn in [5] with reference to the characteristics of rainfall during tropical cyclones in Taiwan. Additionally, the strong precipitation may have been a factor further increasing the wind damage loss in terms of trees fell as a combined result of wind forcing and decrease of the binding strength of soil because of frequent precipitation. The precipitation triggered by the cyclonic storm gave rise to atmospheric cooling (Fig. 8), with the largest cooling (3.5 °C) at Karwar, Malpe, and Dona Paula and the least (3°C) at Ratnagiri.

C. Significant Wave-Height Intensification

The activated surface wind speed in association with Phyan caused intensified sea surface wave conditions all along the west India coastal waters. The highest significant wave height of 3.2 m occurred at Karwar and Panaji, followed by Ratnagiri with 2.7 m. All other locations exhibited ~2 m significant wave height. Coastal water regions of the sea are characterized by complex geometry (bathymetry, shape of land-sea interface, etc) and dynamics (e.g., current pattern), all of which may play a role in the sea surface wave characteristics. It may be noted that Karwar, Panaji, and Ratnagiri regions (offshore of which the maximum significant wave heights were observed) have corrugated coastal topography. Wave focusing and amplification caused by the curvature of the land-sea interface could be a particularly important factor that influences the wave heights at these coastal water bodies. Karwar and Panaji are additionally qualified by the outfall from the Kali River and Mandovi-Zuari estuarine network, respectively. The observed additionally intensified significant wave heights at these two coastal water bodies might have been caused by the wave-current interaction driven by the strong precipitation-induced downstream current from these rivers.

D. Sea Surface Cooling

Phyan caused drop in SST at several coastal water regions, with the largest drop (5.5° C) at Calicut and the smallest at Kanyakumari and Porbander. One of the reasons for the observed drop in SST during the passage of the cyclone could be the cooler subsurface water brought to the surface as a result of the stirring of the upper ocean layers by the high winds associated with the cyclone or removal of heat from the ocean surface through its action of vertical redistribution of heat. The cyclone-driven surface wind near Calicut region was ~5 m/s (See Fig. 2) and this must have in part given rise to the observed sea surface cooling. However, whereas the atmosphere tends to respond almost instantaneously, the sea is expected to react more slowly due to its high heat capacity.

Intensification of sea-surface wave climate could also influence sea surface cooling in part through increased mixing. However, the largest drop in SST occurred at a region where the wave climate was weak, rather than at the regions where the significant wave heights were the maxima (e.g., Karwar, Panaji and Ratnagiri). Thus, several other presently unknown factors such as precipitation- or wind-induced atmospheric cooling, upwelling etc., appears to have given rise to the observed sea surface cooling.

E. Storm Surge

An abnormal sea level rise caused by strong tropical storm, known as storm surge, results from strong winds, atmospheric pressure disturbances, rainfall, and sea surface waves and swells associated with the storm. The storm parameters that determine the coastal surge level are the storm characteristics such as (1) central pressure (c_p), (2) storm size (i.e., radius of maximum wind speed [R_{max}]), (3) storm forward velocity [v_f], (4) the angle of storm track relative to the coast (θ), (5) landfall location as well as the storm-wind fields. The rate of change in c_p is reasonably linearly dependent on storm size. Major storms tend to be stronger off the coast and begin to decay before they make landfall, the quantum of decay being site-specific to a given area. The wind fields in cyclones vary considerably during their approach to the shore. Extensive numerical studies have shown that coastal surge levels are very sensitive to storm intensity, typically categorized by pressure differential defined as the peripheral pressure minus central pressure (i.e., $\Delta p = p_0 - c_p$, where p_0 is the peripheral pressure), storm size (i.e., R_{max} or R_p), and storm location relative to a site. However, based on the results of sensitivity studies, storm surge is less sensitive to θ and v_f (during approach to land). It has been reported that characteristic variations of coastal surges as a function of Δp , θ , and v_f tend to be quite smooth with either linear or slightly curved slopes [6]. For a given location, a major portion of the surge response to the cyclone is captured by the variation of Δp and R_p [7].

The total coastal sea-level elevation is the combined effect of storm surge, wave set-up, and tidal elevation; together with the non-linear interaction of wind-waves and tides with the storm surge. Locally generated seiches can also contribute elevation changes of order 1 m at some stations. As observed in [8] and more recently in [9, 10], the non-linear interaction of surge and tide may significantly modify the evolution of surges. However, based on numerical experimental results, it has been reported that although there may be some degree of nonlinearity in the superposition of tides and storm surges, linear superposition provides a reasonable estimate of the (nonlinearly) combined effects of tides and surges [6]. All the locations from which sea level measurements during the passage of Phyan are available in the present study are tidally dominated regions. Following conventional practice, we first decomposed the instantaneous sea level (η) into a tidal (η_T) and residual (η_R) component, so that $\eta = \eta_T + \eta_R$

Tide is deterministic, and given its harmonic constants, it is readily predictable for any period. The residual includes the contribution of phenomena such as storm surges and harbour

seiches; together with the effect of observation and tidal prediction errors. In general, there exists a transfer function between atmospheric forcing and the sea level response. The observed surge heights at the coastal locations considered in the present study are in agreement with the barometric pressure drop, with the larger surge corresponding to the larger pressure drop (See Figs 5 and 9). Both Karwar and Goa, which experienced the largest significant wave height, exhibited the largest surge (See Figs. 3 and 9) thereby indicating the role of wave set-up in the surge generation at these locations. Analysis of surges associated with hurricanes *Katrina* and *Rita* provided convincing indications that waves contribute significantly to coastal surges [6] primarily because of wave-driven water mass transport [11] and radiation stress from wave fields [12]. Other factors that influence coastal surges are wave-current interactions, coastal bathymetry and landforms.

The evolution of storm surges near the coast is known to be very sensitive to the coastal geometry and offshore bathymetry. This is seen in our measurements from several locations during Phyan. The wind flow at the west India coastal waters during Phyan was northwesterly, thus possessing a landward-oriented cross-shore component and an equator-ward alongshore component. Whereas the former supports piling up of water on the west India coast, the latter supports piling down at this coast by virtue of Coriolis force trying to deflect the water mass to the west. Thus, the effective wind-driven surge at this coast is a manifestation of these two opposing effects (i.e., piling up and piling down) if the land-sea interface is continuous (i.e., devoid of breaks). In the present study Malpe, Karwar, and Goa, which are the three coastal locations from which sea-level measurements are available, are estuarine sites which communicate with the Arabian Sea. These estuaries have given rise to breaks in the coast, thereby providing an additional path for the water to escape into the river, instead of getting piled up. However, these estuaries also provide the requisite pathways for the discharge of appreciable quantity of fresh water supplied by the heavy precipitation associated with the cyclone and carried by the rivers into the sea. Further, since the regions under the present study fall under the influence of freshwater runoff from major rivers and river systems, the influx brought by them operates as a buoyancy input which influences the baroclinic effects and therefore impacts the surge. Although the rainfall at Karwar during Phyan was larger than that at Goa, the latter witnessed the largest surge because the combined river discharge there from two large rivers (Mandovi and Zuari) was much larger than that at Karwar from a single river (Kali). Thus, the combinations of several opposing effects have contributed to the evolution of the observed surges. Despite the intense wind forcing, Kavaratti Island lagoon experienced weak surge because of lack of river influx and absence of a large land boundary for piling up to occur.

IV. CONCLUSIONS

The present study aimed at providing some insight on the synoptic evolution and some meteorological and oceanographic impacts of the cyclonic storm Phyan, which swept approximately in a northeastward direction along the eastern Arabian Sea between 9 and 12 November 2009 and caused considerable fatalities and economic/environmental damage along the west India coastal and offshore waters. The cyclonic storm Phyan was attended by strong winds and gusts, atmospheric pressure disturbances, intense rainfall, and atmospheric cooling at several regions. It was found that atmospheric forcing exerted considerable influence on sea level in terms of intensified sea surface waves and increased coastal surge levels. The observed surge heights at the coastal locations considered in the present study are in broad agreement with the barometric pressure drop (with the larger surge corresponding to the larger pressure drop), discharge of appreciable quantity of fresh water supplied by the heavy precipitation and carried by the rivers into the sea, as well as coastal wave-setup generated by intensified wave height. Other factors that influenced coastal surges are coastal bathymetry and landforms, and possibly even wave-current interactions. Thus, the combinations of several factors such as (i) water piling up at the coast supported by seaward flow of the excess water in the rivers due to heavy rains and water mass transport by westerly cross-shore wind and waves, (ii) water piling down at the coast supported by the northerly alongshore wind (by virtue of Coriolis effect) and upstream penetration of seawater into the rivers, and (iii) possible interaction of upstream flow with river runoff, together resulted in the observed surge flooding at the west India coast. Despite the intense wind forcing, Kavaratti Island lagoon experienced insignificantly weak surge (~7 cm) because of lack of river influx and absence of a sufficiently large land boundary required for the sustenance of wave/wind-driven water mass transport which tends to pile up at the land-sea interface.

The observed surges neither at the mainland coast nor at the islands were large enough to cause fatalities. It is proposed that large sea surface waves triggered by intensified wind speed and gust together with uprooting of trees as a combined result of enhanced wind forcing and decrease of the binding strength of soil because of frequent precipitation have been factors that gave rise to the fatalities (particularly fishermen) and damage in the wake of the tropical cyclonic storm Phyan.

ACKNOWLEDGMENT

We are grateful to Dr. K.V. Radhakrishnan (PG Center for Marine Biology, Karnataka University, Kodibag, Karwar) for supplying rainfall data from Malpe and Karwar.

REFERENCES

- [1] L.W. Uccellini, "Process contributing to the rapid development of extratropical cyclones", In: Extratropical cyclones: The Eric Palmen memorial volume, edited by: Newton, C., and E. Holopainen, *Am. Meteorol. Soc.*, pp. 81-107, 1990.
- [2] A.H. Fink., T. Brucher, V. Ermert, A. Kruger, and J.G. Pinto, "The European storm Kyrill in January 2007: synoptic evolution,

- meteorological impacts and some considerations with respect to climate change”, *Nat. Hazards Earth Syst. Sci.*, vol. 9, pp. 405-423, 2009.
- [3] M.Lonfat, F.D. Marks Jr., and S.S. Chen, “Precipitation distribution in tropical cyclones using the Tropical Rainfall Measuring Mission (TRMM) microwave imager: A global perspective”, *Mon. Weather Rev.*, vol. 132, pp. 1645-1660, 2004.
- [4] J.C.L. Chan, K.S. Liu, S.E. Ching, and E.S.T. Lai, “A symmetric distribution of convection associated with tropical cyclones making landfall along the South China coast”, *Mon. Weather Rev.*, vol. 132, pp. 2410-2420, 2004.
- [5] K.K.W. Cheung, L.-R. Huang, and C.-S. Lee, “Characteristics of rainfall during tropical cyclone periods in Taiwan”, *Nat. Hazards Earth Syst. Sci.*, vol. 8, pp. 1463-1474, 2008.
- [6] D.T. Resio., J. Irish, and M. Cialone, “A surge response function approach to coastal hazard assessment — part 1: basic concepts”, *Nat. Hazards*, vol. 51, pp. 163-182. DOI:10.1007/s11069-009-9379-y, 2009.
- [7] J.L. Irish., D.T. Resio, and J.J. Ratcliff, “The influence of storm size on hurricane surges”, *J. Phys. Oceanogr.*, vol. 38, pp. 2003-2013, 2008.
- [8] B. Johns, A.D. Rao, S.K. Dube, and P.C. Sinha, “Numerical modeling of the tide surge interaction in the Bay of Bengal”, *Philos. Trans. R. Soc. Lond.* Vol. A 313: pp. 507-535, doi:10.1098/rsta.1985.0002, 1985.
- [9] P.C. Sinha, Y.R. Rao, S.K. Dube, and A.D. Rao, “Numerical investigation of tide-surge interaction in Hooghly Estuary, India”, *Mar. Geod.*, vol. 19: pp. 235-255, doi:10.1080/01490419609388082, 1996.
- [10] P.C. Sinha., I. Jain, N. Bhardwaj, A.D. Rao, and S.K. Dube, “Numerical modeling of tide-surge interaction along Orissa coast of India”, *Nat. Hazards*, vol. 45:pp. 413-427, doi:10:1007/s11069-007-9176-4, 2008.
- [11] M.S. Longuet-Higgins, “Mass transport in water waves”, *Philosophical Transactions of the Royal Society of London*, vol. 245, pp. 535-581, 1953.
- [12] M.S. Longuet-Higgins and R.W. Stewart, “Radiation stresses in water waves; a physical discussion, with applications”, *Deep-Sea Res.*, vol. 11, pp. 529-562, 1964.